Macromolecules
ARTICLE

Macromolecules **2009**, *42*, 7863–7876 **7863**
DOI: 10.1021/ma9009802

Glass Transition Breadths and Composition Profiles of Weakly, Moderately, and Strongly Segregating Gradient Copolymers: Experimental Results and Calculations from Self-Consistent Mean-Field Theory

Michelle M. Mok,[†,&] Jungki Kim,[‡,&] Christopher L. H. Wong,[†] Stephen R. Marrou,[‡] Dong Jin Woo,[‡,∥] Christine M. Dettmer,[§] SonBinh T. Nguyen,[§] Christopher J. Ellison,[⊥] Kenneth R. Shull,[†] and John M. Torkelson*[,‡,†]

[†]*Department of Materials Science and Engineering and* [‡]*Department of Chemical and Biological Engineering and* [§]*Department of Chemistry, Northwestern University, Evanston, Illinois 60208,* [∥]*Department of Molecular Science and Technology, Ajou University, Suwon 443-749, Korea, and* [⊥]*Department of Chemical Engineering and Materials Science, University of Minnesota, Minneapolis, Minnesota 55455.* [&]*Cofirst authors.*

Received May 5, 2009; Revised Manuscript Received September 24, 2009

ABSTRACT: Gradient copolymers are prepared from comonomer systems with a range of segregation strengths and homopolymer glass transition temperature (T_g) differences to explore the breadths that can be achieved by their single, continuous glass transition regions compared to random and block copolymers. A variety of chain architectures are synthesized using semibatch nitroxide-mediated controlled radical polymerization, including linear gradients, sigmoidal gradients, blocky gradients, and blocky random cases. The derivative of the differential scanning calorimetry heat curve is used to extract T_g breadths (ΔT_gs). For the first time, these T_g breadths are compared against values derived from nanophase separation levels predicted by self-consistent mean-field theory and found to be in good accord. In moderately segregating systems (styrene (S)/*n*-butyl acrylate and S/*tert*-butyl acrylate), ΔT_g may be tuned dramatically via gradient structure and molecular weight; e.g., a T_g breadth exceeding 100 °C, or >65% of the homopolymer T_g difference, is obtained with a sigmoidal gradient copolymer of S/*n*-butyl acrylate. In the very weakly segregating system (S/*n*-butyl methacrylate), ΔT_g remains narrow (<40% of the homopolymer T_g difference), regardless of gradient design. In strongly segregating systems (S/4-vinylpyridine and S/4-acetoxystyrene (AS)), ΔT_gs are observed spanning 70−80% of the homopolymer T_g difference. Small-angle X-ray scattering applied to S/AS materials demonstrates a range of temperature-sensitive scattering intensities consistent with the level of segregation observed through their ΔT_gs.

Introduction

Since the inception of controlled radical polymerization (ContRP)[1−3] more than 15 years ago, this approach has led to the relatively simple synthesis of a variety of novel polymers and copolymers.[4−6] In particular, gradient copolymers,[7−43] a class of copolymer in which the comonomer composition gradually varies along the chain length and that cannot be made by conventional radical polymerization (ConvRP) (perhaps better known as "free radical polymerization"), can be easily synthesized by ContRP, owing to its combined pseudoliving character and generally facile cross-propagation of radicals compared to anionic copolymerization.[7−20,22,23,25−35] (Other (pseudo)-living polymerization methods that can have effective cross-propagation, including ring-opening metathesis polymerization[36] and cationic polymerization, may also be used to make gradient copolymers. Copolymers having gradient character may also be made from several types of monomers via anionic polymerization[21,24] using carefully designed semibatch reactions to counteract the highly unfavorable cross-propagation in anionic polymerization.[7]) Gradient copolymers have sequence distributions along the chains that are intermediate in character to diblock copolymers, which have a step change in comonomer composition, and random copolymers (statistical copolymers),[37] which exhibit no variance in average local composition along their chains.[7,38−41] Because of their unusual molecular structure, gradient copolymers have efficacy as cosmetics additives,[42] emulsion stabilizers,[43] compatibilizers for immiscible blends,[28−31,35] filler dispersant for nanocomposites,[44] and vibration or acoustic damping materials.[34]

For comonomers with repulsive enthalpic interactions, theory has predicted the presence of microphase or nanophase separation in gradient copolymer melts related to that of diblock copolymers, but with a few unique features.[38−41] While the critical χN value or $(\chi N)_c$ (where χ is the Flory−Huggins interaction parameter between comonomers and N is the average number of monomers per chain) for a compositionally symmetric diblock copolymer is 10.495,[45] that of a linearly tapered gradient copolymer is predicted to have a value of 29.25[40] or 29.55.[41] For gradient copolymers with sigmoidal compositional profiles between the linear gradient and block cases, the value of $(\chi N)_c$ decreases toward the value for the block case as the profile grows more block-like.[41] For A/B gradient copolymers with chain ends that do not extend to pure A and pure B compositions, $(\chi N)_c$ can shift to values greater than 30.[41]

These same studies have predicted that compositional profiles within ordered gradient copolymers remain sinusoidal, even in systems well above their critical point of separation.[40,41]

*To whom correspondence should be addressed. E-mail: j-torkelson@northwestern.edu.

Published on Web 10/02/2009

The amplitude of the sinusoidal function grows as χN increases to give increasingly A-rich and B-rich regions, but never fully segregates to the step-function profile typically seen in diblock copolymer melts. For example, a linear A/B gradient copolymer with $\chi N \sim 40$ has A-monomer volume fraction profiles varying between $\phi_A \sim 0.25$ and 0.75; at $\chi N \sim 140$, ϕ_A varies between ~0.15 and 0.85.[41] As a result, A/B gradient copolymers have been predicted to possess unique thermal properties,[12] such as extremely broad glass transition regions when the glass transition temperatures (T_gs) of the two related homopolymers differ significantly.[31] One would also expect that these properties can be manipulated through variation of segregation strength (χ), molecular weight or chain length (N), and gradient profile (related to the critical value of χN).

Numerous studies have used differential scanning calorimetry (DSC) to characterize thermal properties of gradient copolymers.[17−28,31,33] Most studies reported single glass transition regions, similar to random copolymers, but sometimes suggested that these regions covered broader temperature ranges than those in random copolymers. In 2006, our group[31] reported an analysis technique to quantify gradient copolymer glass transition breadth systematically as a function of gradient development in copolymers prepared from very strongly segregating styrene/4-hydroxystyrene (S/HS) comonomers. (Edgecombe et al.[46] estimated that χ = ~6 for the S/HS system.) In these materials, the temperature range separating fully glassy and fully rubbery behavior spanned ~80−90% of the region between the T_gs of polystyrene (PS) and poly(4-hydroxystyrene) (PHS); T_g(PHS) − T_g(PS) = ~90 °C. In 2007, we used the same method to demonstrate that styrene/acrylic acid (S/AA) gradient copolymers can exhibit T_g breadths exceeding the difference between the T_gs of the relevant homopolymers; this can be explained by more effective hydrogen bonding between AA units when AA units have neighboring S units along the chain backbone.[33] Recently, we used dynamic mechanical analysis to show that in more weakly segregating S/*n*-butyl acrylate (S/nBA) gradient copolymers the damping breadth, which is related to T_g breadth, can be tuned via the strength of the composition gradient.[34]

Here, we provide an extensive analysis of achievable T_g breadth in gradient copolymers possessing different segregation strengths, homopolymer T_g differences, and gradient architectures. For the first time, experimental T_g breadths obtained via differential scanning calorimetry are compared to predictions of T_g breadths based on the calculated sinusoidal composition profiles obtained from applying self-consistent mean-field (SCMF) techniques to these materials. We have studied the following copolymer systems: the weakly to moderately segregating systems of S/nBA (χ reported as 0.034[47] and 0.087,[48] T_g(PS) − T_g(PnBA) = ~150 °C[49,50]) and S/*tert*-butyl acrylate (S/*t*BA, χ estimated by us to be 0.09,[51−54] T_g(PS) − T_g(PtBA) = ~60 °C[49]); the very weakly segregating system of S/*n*-butyl methacrylate (S/BMA, χ reported as 0.012−0.015[55] and 0.017−0.018,[56] T_g(PS) − T_g(PBMA) = ~80 °C[49]); and the very strongly segregating systems of S/4-vinylpyridine (S/4VP, χ reported as 0.30−0.35,[57] T_g(P4VP) − T_g(PS) ~45 °C[58]) and S/4-acetoxystyrene (S/AS, χ estimated by us to be 0.45,[51−54] T_g(PAS) − T_g(PS) = ~30 °C[31]). Synthesis involved semibatch, nitroxide-mediated ContRP, and different gradient architectures were prepared by varying the rates at which the monomers were introduced during the semibatch reactions. The T_g breadths of the copolymers were characterized using the DSC approach described in refs 31 and 33 and compared to those obtained for related random and block copolymers. To compare the level and temperature dependence of microphase or nanophase segregation obtained in gradient copolymers to those observed in diblock copolymers, small-angle X-ray scattering (SAXS) was performed for a family of S/AS copolymers.

Table 1. Summary of Glass Transition Temperature Data (±0.5 °C) for S/nBA (Figure 2), S/tBA (Figure 4), and S/BMA (Figure 5) Copolymers

sample	F_S	M_n (g/mol)[a]	T_o (°C)	ΔT_g (°C)
S*block*NBA46	0.46	96 500	−57.5	17.5
			97.5	14.0
S*ran*NBA55	0.55	95 100	15.7	18.6
S*ran*NBA66	0.66	80 200	32.0	21.0
S*grad*NBA59	0.59	96 900	7.1	53.9
S*grad*NBA62	0.62	95 100	−16.2	101.2
S*ran*TBA46	0.46	172 900	62.8	14.8
S*block*TBA54	0.54	61 300	39.5	14.9
			97.5	14.4
S*grad*TBA53	0.53	135 100	65.6	39.6
S*ran*TBA67	0.67	93 200	70.7	15.0
S*block*TBA69	0.69	83 200	37.7	16.6
			96.8	15.0
S*grad*TBA67	0.67	85 200	69.0	35.4
S*ran*BMA75	0.75	61 700	50.5	20.1
S*grad*BMA71	0.71	83 000	52.1	33.7
S*grad*BMA49	0.49	57 800	40.1	20.7

[a] The M_n values for the random and gradient copolymers were characterized by GPC relative to PS standards using THF as the eluent. The block copolymer M_n values were calculated from the M_n of macroinitiators, as measured by GPC using universal calibration with PS standards, and their final comonomer compositions as measured by ^{1}H NMR.[88]

Experimental Section

Materials and Methods. Monomers (Aldrich) were deinhibited using inhibitor removers and dried over CaH_2 before use. The inhibitor removers used were Aldrich 31,134-0 (for items inhibited with *tert*-butyl catechol) and Aldrich 311332 (for items inhibited with hydroquinone and monomethyl ether hydroquinone). The initiators benzoyl peroxide (BPO; Aldrich) and 2,2′-azobis(isobutyronitrile) (AIBN; Pfaltz and Bauer) were used as received. The unimolecular initiator alkoxyamine 29 (A29)[6,29−31] (2,2,5-trimethyl-3-(1-phenylethoxy)-4-phenyl-3-azahexane) was synthesized previously and is the same material as that used in refs 29−31. The unimolecular initiator BlocBuilder[59−61] (*N*-(2-methylpropyl)-*N*-(1-diethylphosphono-2,2-dimethylpropyl)-*O*-(2-carboxylprop-2-yl)hydroxylamine, 99%) was kindly supplied by Arkema, Inc.

Copolymer compositions were measured by ^{1}H NMR spectroscopy (Varian Inova 500 MHz) using $CDCl_3$ as solvent. The peak intensity from the spectra associated with the aromatic hydrogens (from styrene units; m, 6.2−7.3 ppm) was compared to the intensity associated with all other hydrogens (m, 0.6−4.5 ppm) to determine the copolymer composition. The apparent number-average molecular weight (M_n) and the dispersity[62] (also referred to as the "polydispersity index" or PDI) for the random and gradient copolymers were characterized by gel permeation chromatography (GPC, Waters Breeze) relative to PS standards using tetrahydrofuran (THF) as the eluent. For S/4VP copolymers, molecular weight data are not reported since the samples interacted with the GPC columns. The block copolymer M_n values were calculated from the M_n of macroinitiators, as measured by GPC using universal calibration with PS standards, and their final comonomer compositions, as measured by NMR. The copolymer syntheses and characterizations are summarized in Tables 1−4 and the Supporting Information.

Synthesis of Random Copolymers. Sets of random copolymers, with at least seven samples per set, spanning a range of styrene mole fractions (F_S) were prepared by batch ConvRP using AIBN as initiator (see Supporting Information for reactivity ratios and full synthesis details). Reactions for S/4VP, S/nBA, S/tBA, and S/AS were performed at 70−80 °C while the S/BMA sets were carried out at 90 and 105 °C.[63] For the S/nBA, S/tBA, S/4VP, and S/AS copolymer systems, random copolymers were also synthesized from both ContRP ([BlocBuilder] = 1.3×10^{-3} mol/L) and

Table 2. Summary of Glass Transition Temperature Data (±0.5 °C) for S/nBA Gradient Copolymer Aliquots (Figure 3)

sample		F_S	M_n (g/mol)[a]	T_o (°C)	ΔT_g (°C)
S*grad*NBA59	2.0 h	0.74	44 200	47.4	26.2
	4.0 h	0.65	75 400	24.7	37.8
	6.0 h−final	0.59	96 900	7.1	53.9
S*grad*NBA62	2.0 h	0.85	39 800	62.1	26.9
	4.0 h	0.78	56 800	41.3	40.8
	6.0 h	0.70	79 900	1.9	81.2
	8.0 h	0.65	88 400	−13.0	96.1
	9.0 h−final	0.62	95 100	−16.2	101.2
S*grad*NBA73	2.0 h	0.89	12 300	74.5	19.6
	4.0 h	0.78	25 700	50.5	27.8
	5.0 h	0.75	33 700	37.7	32.8
	6.0 h−final	0.73	40 700	32.6	37.0

[a] The M_n were characterized by GPC relative to PS standards using THF as the eluent.[88]

Table 3. Summary of Glass Transition Temperature Data (±0.5 °C) for S/4VP Copolymers (Figure 6)[a]

sample	F_S	T_o (°C)	ΔT_g (°C)
S*ran*4VP40	0.40	128.2	12.3
S*ran*4VP22	0.22	138.3	12.0
S*grad*4VP23	0.23	119.0	31.7
S*grad*4VP33	0.33	116.0	35.1

[a] For S/4VP copolymers, molecular weight data are not reported since the samples interacted with the GPC columns.

Table 4. Summary of Glass Transition Temperature Data (±0.5 °C) for S*grad*AS64 Aliquots (Figure 7a) and S/AS Blocky Gradient[a], Blocky Random,[a] and Block Copolymers (Figure 7b)

sample	F_S	M_n (g/mol)[b] [PS block M_n]	T_o (°C)	ΔT_g (°C)
S*grad*AS64				
2.0 h	0.80	34 000	101.2	14.0
3.0 h	0.75	39 100	100.5	18.4
4.0 h	0.70	49 200	101.9	21.8
5.0 h	0.64	51 300	105.2	21.5
S*bgrad*AS84	0.84	58 800 [41K]	98.7	13.1
S*bran*AS81	0.81	55 600 [34.1K]	99.8	13.3
S*bran*AS78	0.78	48 100 [34.1K]	98.7	12.7
			111.4	15.3
S*bran*AS72	0.72	50 700 [34.1K]	99.2	13.1
			112.3	18.7
S*block*AS67	0.67	60 300 [34.1K]	99.7	12.5
			112.2	19.8

[a] With blocky gradient and blocky random copolymers, the following example applies regarding the molecular structures. With S*bgrad*AS84, the copolymer has an S block with M_n = 41 000 g/mol, an overall apparent M_n = 58 800 g/mol (by GPC relative to PS standards), and an overall S mole fraction of 0.84. [b] The block copolymer M_n value was calculated from the M_n of macroinitiator and its final comonomer composition as measured by NMR. The M_n for the random and gradient copolymers were characterized by GPC relative to PS standards using THF as the eluent.[88]

ConvRP ([AIBN] = 5.5×10^{-2} mol/L) at 90 °C using comonomer reaction mixtures targeting $F_S \sim 0.50$ to determine whether the polymerization type had any impact on T_g breadth or value. Sets of S/BMA random copolymers were also prepared using ContRP ([BlocBuilder] = 5.2×10^{-3} mol/L) at both 90 and 105 °C. The copolymers were washed by several cycles of dissolution in THF and precipitation into methanol and dried under vacuum, except some S/4VP copolymers which were washed by cycles of precipitation into hexanes and dissolution in THF. Initiator concentrations were chosen to yield M_n > 40 000 g/mol, and reaction times were limited to maintain low conversion in order to prevent drift of the monomer mix composition. See Supporting Information for results and molecular characterization of all random copolymer sets.

Synthesis of Diblock Copolymers. Block copolymers were synthesized by sequential batches of nitroxide-mediated ContRP. For the synthesis of an S/nBA block copolymer with a F_S = 0.46 (S*block*NBA46), a PnBA macroinitiator was synthesized using nBA (10.0 mL, 0.070 mol) and A29 (5.23×10^{-3} mol/L) at 120 °C for 180 min under N_2. This PnBA (M_n = 57 000 g/mol; PDI = 1.60) was combined with S (5.0 mL; [PnBA] = 3.42×10^{-3} mol/L) in a test tube and placed in an oil bath at 120 °C for 70 min under N_2. The resulting diblock copolymer (F_S = 0.46) was washed and dried as described above.

For the S/tBA system, a PtBA macroinitiator was prepared by combining tBA and A29 (1.12×10^{-2} mol/L) and polymerizing at 115 °C for 60 min. The macroinitiator (M_n = 31 400 g/mol; PDI = 1.95) was dissolved into a test tube charged with S ([PtBA] = 2.68×10^{-3} mol/L) and placed in a bath at 115 °C under N_2 for 60 min to yield a S/tBA block copolymer with F_S = 0.69. In a separate test tube, styrene was combined with the PtBA macroinitiator ([PtBA] = 5.42×10^{-3} mol/L) and heated at 115 °C for 60 min to obtain a diblock copolymer with F_S = 0.54.

For the S/AS system, a PS macroinitiator was prepared by combining S and BlocBuilder (3.00×10^{-3} mol/L) in a test tube, purging for 30 min with N_2 and reacting at 90 °C for 2.25 h. The resulting material (M_n = 34 100 g/mol, PDI = 1.36) was chain extended with AS ([PS] = 2.00×10^{-3} mol/L) at 100 °C for 90 min to create a pure diblock copolymer (S*block*AS67, M_n = 60 300 g/mol) or mixtures of S and AS to create "blocky random" (S*bran*AS) copolymers[35] where the second block is a random combination of S and AS ([PS] = $(2.2-2.6) \times 10^{-3}$ mol/L, 100 °C for 60 min). Three blocky random cases were synthesized, with the S:AS molar ratios of the chain extension mixtures being 3:1 for S*bran*AS81 (M_n = 55 600 g/mol), 1:1 for S*bran*AS78 (M_n = 48 100 g/mol), and 1:3 for S*bran*AS72 (M_n = 50 700 g/mol).

Synthesis of Gradient Copolymers. Semibatch ContRP processes, using A29 or BlocBuilder as the unimolecular initiator, were employed in the preparation of gradient copolymers. For each polymerization, the starting monomer was first combined with the initiator and placed into a heated oil bath under continuous N_2 purging, while the secondary monomer was continuously added to the reactor via a syringe pump. In order to verify the formation of a composition gradient, aliquots (~1 mL) of the reaction mixture were collected throughout the polymerization process. See Supporting Information for a summary of synthesis details and proof of compositional gradient formation for all gradient copolymers synthesized in the current study.

For the S/nBA gradient copolymer with F_S = 0.59 (S*grad*NBA59), S (10.0 mL, 0.087 mol), and A29 (3.92×10^{-3} mol/L) were combined in a test tube and purged with N_2 for 30 min. To this test tube, nBA monomer was delivered at a constant flow rate (4.0 mL/h) during the entire ContRP process at 120 °C under N_2 purging. The copolymers in the aliquot samples were isolated by precipitation into methanol followed by filtration. Each filtered copolymer was dissolved in THF and precipitated into methanol again and dried under vacuum before characterization via GPC and ^{1}H NMR. Finally, the copolymerization was stopped at 6.0 h, and the resulting copolymer (S*grad*NBA59) was isolated and washed as described above.

To synthesize the S/nBA gradient copolymer with F_S = 0.62 (S*grad*NBA62), S (10.0 mL, 0.087 mol) and A29 (3.92×10^{-3} mol/L) were combined in a test tube and purged with N_2 for 30 min. The nBA monomer was delivered at a flow rate that increased from 2.0 mL/h by 2.0 mL/h every 3.0 h during the entire 9.0 h semibatch ContRP process, at 120 °C under N_2. To synthesize the S/nBA gradient copolymer with F_S = 0.73 (S*grad*NBA73), a similar increasing rate of monomer feed was used. BlocBuilder initiator (7.87×10^{-3} mol/L) was mixed with S (10.0 mL, 0.087 mol) in a test tube and heated at 100 °C for 6.0 h, with nBA added at a rate of 1.0 mL/h and increasing by 2.0 mL/h every 2.0 h for the full 6.0 h of the reaction.

Two S/tBA gradient copolymers were prepared. The initiator A29 (5.61×10^{-3} mol/L) was mixed with styrene (7.0 mL, 0.061 mol), and tBA was added to the reactor at a rate of 5.0 mL/h for 6.0 h for the gradient copolymer with $F_S = 0.53$ (S*grad*TBA53). The addition rate of tBA was reduced to 3.5 mL/h for the gradient copolymer with $F_S = 0.67$ (S*grad*TBA67).

Two S/BMA gradient copolymers were also made using A29. For the synthesis of an S/BMA gradient copolymer with $F_S = 0.71$ (S*grad*BMA71), S (10.0 mL, 0.087 mol) was mixed with A29 (5.23×10^{-3} mol/L) in a test tube and heated at 115 °C for 180 min with BMA being added at a rate of 3.0 mL/h. For an S/BMA gradient copolymer with $F_S = 0.49$ (S*grad*BMA49), a mixture of S (5 mL, 0.044 mol) and A29 (1.05×10^{-2} mol/L) was polymerized for 130 min while BMA was added at a rate of 4.0 mL/h.

The S/4VP gradient copolymers were synthesized using BlocBuilder as initiator. For the $F_S = 0.23$ case (S*grad*4VP23), BlocBuilder (2.62×10^{-3} mol/L), 4VP monomer (10.0 mL, 0.093 mol), and *N*,*N*-dimethylformamide (3.0 mL) were combined in a test tube. The mixture was heated at 90 °C for 5.0 h with styrene being added at a rate of 5.0 mL/h. The same reaction conditions were used for the $F_S = 0.33$ gradient case (S*grad*4VP33), except that the reaction temperature was increased to 95 °C at 1.5 h and finally to 100 °C at 3.0 h. All S/4VP copolymers were washed by cycles of precipitation into hexanes and dissolution in THF.

The synthesis details for the S/AS gradient copolymer ($F_S = 0.64$) were reported in ref 7. An S/AS blocky gradient copolymer was also prepared. First, a PS macroinitiator ($M_n = 41\,000$ g/mol, PDI = 1.40) was synthesized from BlocBuilder and S (2.22×10^{-3} mol/L, 2.0 h at 100 °C). The recovered PS macroinitiator (0.77 g) was then redissolved in S (3.6 mL) and purged with N_2 for 30 min before immersion into an oil bath at 100 °C. The AS monomer was added continuously at a rate of 3.2 mL/h for 90 min to give a material with final $F_S = 0.84$.

Thermal Property Characterization. Thermal analysis was done with a differential scanning calorimeter (Mettler-Toledo DSC 822e) calibrated with indium and zinc standards. Dry N_2 was passed through the DSC cell during measurement. Samples were heated to at least 30 °C above their component glass transitions and held at that temperature for 30 min to erase thermal history. Each sample was then cooled below its component glass transitions at a rate of 40 °C/min and reheated at a rate of 10 °C/min (second heat). Glass transition breadth data were extracted from the second heat scan. All measurements were repeated twice.

Small-Angle X-ray Scattering. Temperature-dependent SAXS was done on S/AS copolymers, which were consolidated by compression molding and annealed at 200 °C for 2.0 h. X-rays (0.154 nm) were generated from a rotating Rigaku Ru-200BVH copper anode using a 0.2×2.0 mm^2 microfocus cathode and were monochromatized by Franks mirrors and a nickel foil filter. The samples were 441 cm (distance calibrated with duck tendon) from a 2-D Siemens HI-STAR detector which measured the intensity of scattered X-rays as a function of scattering angle (θ). The samples were first annealed at 200 °C for 5 min and then cooled to target temperatures (120, 160, or 200 °C) and annealed for 5 min before SAXS data were collected. The 2-D scattering data were azimuthally averaged to produce plots of intensity versus the magnitude of the scattering wave-vector modulus $q = |q| = (4\pi/\lambda)\sin(\theta/2)$, where θ is the scattering angle.

Self-Consistent Mean-Field Technique. Composition profiles were calculated via the SCMF approach developed by Shull[64,65] and Lefebvre et al.[40] for block and gradient copolymers.

Results and Discussion

A. Characterization of the Composition Gradient in Gradient Copolymers. Proof of formation of all gradient structures is provided in the Supporting Information and in Figure 1 for selected copolymers.[66] For all (meth)acrylate cases, the starting comonomer was always styrene (S), and the (meth)acrylate was continuously added into the reactor in order to produce a composition gradient along the copolymer chains. The intermediate copolymers collected as aliquot samples during each polymerization were isolated and characterized via GPC and ^{1}H NMR to obtain apparent molecular weights (MW) and cumulative styrene mol fractions (F_S). The evolution of F_S as a function of the apparent normalized chain length (ratio of M_n of each intermediate copolymer to M_n of the full gradient copolymer) is shown in Figure 1. In each case, a decrease in F_S is seen with increasing chain growth due to decreasing S concentration in the comonomer mixture; this is evidence that copolymers indeed have composition gradients.

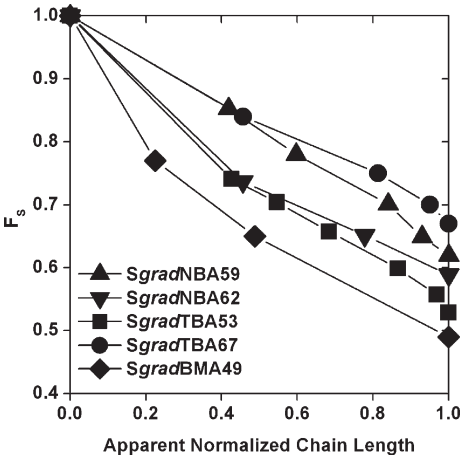

Figure 1. Cumulative styrene mole fraction (F_S) as a function of apparent normalized chain length for selected gradient copolymers.

Because of the diversity of copolymers studied here, we will use a simplified notation for each copolymer. For example, a gradient copolymer of S/nBA with $F_S = 0.59$ will be designated as S*grad*NBA59, a random copolymer of S/tBA with $F_S = 0.67$ will be noted as S*ran*TBA67, and S*block*NBA46 will be used for an S/nBA block copolymer with $F_S = 0.46$.

B. Glass Transition Breadth. Several approaches have been described in the literature to characterize complex thermal behavior of heterogeneous polymeric systems. One method is to determine T_g widths from DSC heat curves by measuring the temperature range over which there is an apparent change in heat capacity from a glassy state to a rubbery state;[67,68] however, this approach does not yield precise results when the T_g is very broad and/or somewhat weak over some temperature range.[69] A second method uses the first derivatives of DSC heat curves with respect to temperature and has been applied in both conventional and temperature-modulated DSC studies of polymer blends,[49,70,71] (multi)block copolymers,[49,72,73] and adsorbed (co)polymers.[74,75] Our recent studies of T_g breadth in S/HS and S/AA gradient copolymers also employed derivatives of DSC curves for effective analysis of T_g breadth.[31,33] In particular, relative to random or block copolymers, uniquely broad T_g responses spanning as much as ~80 °C were observed for the first time from S/HS gradient copolymers. With this method, the T_g breadth (ΔT_g) is defined by the T_g onset (T_o) and T_g end point (T_e) from each derivative curve, where the glass transition is typically manifested by a strong positive peak followed by a small, local minimum due to enthalpy relaxation associated with the nature of the heating protocol in T_g measurements by DSC.

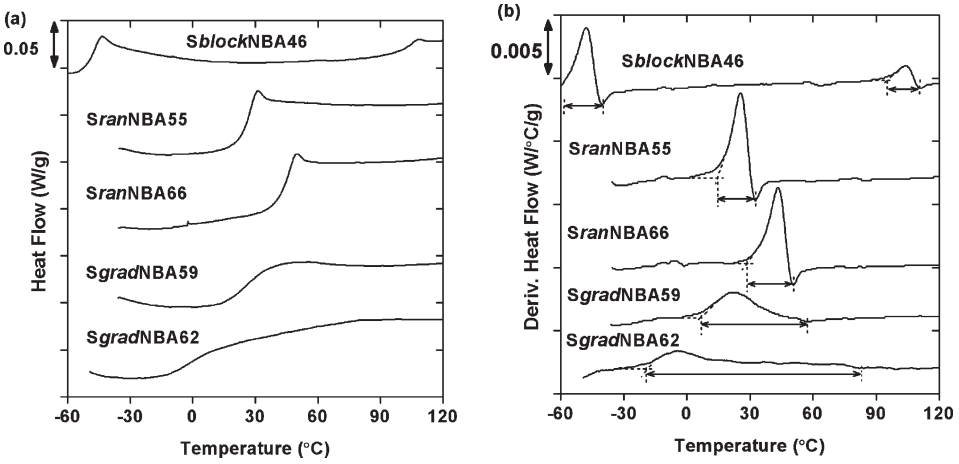

Figure 2. (a) DSC heating curves and (b) derivatives[76] for S/nBA copolymers. From the derivative curve, the value for T_g onset (T_o) is defined by the onset of deviation in the curve from the baseline (e.g., 15.7 °C for S*ran*NBA55), while the T_g end point (T_e) value is defined by the local minimum present due to enthalpic relaxations (e.g., 34.3 °C for S*ran*NBA55). The difference between T_o and T_e yields the T_g breadth (e.g., 18.6 °C for S*ran*NBA55).

We used this analysis technique to compare the T_g values and breadths of S/nBA, S/tBA, S/BMA, S/4VP, and S/AS random copolymers prepared by either ConvRP or ContRP. We found that these were the same within experimental error, so their copolymers prepared using different synthesis techniques are assumed to be comparable in T_g character. Below, we characterize the ΔT_gs from DSC measurements of S/nBA, S/tBA, S/BMA, S/4VP, and S/AS gradient, random, and block copolymers and draw comparisons as a function of comonomer segregation strength and copolymer MW and composition profile.[76]

B.1. S/nBA Copolymers. The original DSC heat curves and derivative curves for a diblock, two random, and two gradient copolymers of S/nBA are shown in Figure 2. The molecular and T_g characterizations are reported in Table 1. The 46/54 mol % S/nBA diblock copolymer (S*block*NBA46) exhibits two distinct peaks in Figure 1b, corresponding to the T_gs of PS and PnBA. This result is consistent with ordered lamellar microphases, each comprised of pure S and pure nBA compositions and is in accord with the study by Miwa et al.,[50] who reported two distinct T_gs from a compositionally symmetric S/nBA diblock copolymer of lower MW (M_n = 35 000 g/mol).

In contrast to S*block*NBA46, S/nBA random and gradient copolymers yield only one discernible glass transition region, but the breadths of T_g among the random and gradient copolymers are vastly different. The ΔT_gs of both S*ran*NBA55 and S*ran*NBA66 are 19−21 °C, similar to what has been observed for homopolymers;[31] such a narrow transition range indicates a lack of nanoscopic heterogeneity, at least over length scales for which DSC provides sensitivity. In contrast, the T_g breadths of S*grad*NBA59 and S*grad*NBA62 are much greater than those of the random copolymers and of each block component in S*block*NBA46. These broad T_g responses can be attributed to the sinusoidal composition profiles expected for nanophase segregated gradient copolymers.[40,41] The inherent compositional heterogeneity along the copolymer chain leads to T_g regions that extend from temperatures representing nBA-rich compositions to temperatures representing S-rich compositions, resulting in an overall broad T_g.

The S*grad*NBA59 and S*grad*NBA62 samples exhibit substantially different ΔT_gs (53.9 °C vs 101.2 °C) despite their similar F_S and M_n values. To address this point, we characterized T_g behaviors of aliquots collected during their semibatch copolymerizations, which can be considered "intermediate" or "partial" gradient copolymer samples (see Figures 3a,b and Table 2). It should be noted that the detailed synthesis schemes between these two gradient copolymers are different. For S*grad*NBA59, we employed a constant addition rate of nBA monomer during the semibatch reaction; for S*grad*NBA62, we increased the rate of nBA addition (i.e., slow, medium, and fast addition rates) as the copolymerization proceeded.

From these reaction schemes, we would expect gradient profiles to be more linear in the constant addition case (S*grad*NBA59) and more sigmoidal in the increasing gradient case (S*grad*NBA62). A sigmoidal profile would lead to larger portions of the chain ends being very S-rich and very nBA-rich compared to the linear case, allowing the phase-segregated material to attain sinusoidal profiles of larger amplitude and hence display a broader T_g. These expected profiles are supported by the relative change in F_S with respect to apparent normalized M_n (Figure 1), where the linear S*grad*NBA59 shows a faster initial incorporation of nBA than the sigmoidal S*grad*NBA62, but the sigmoidal S*grad*NBA62 "catches up" as the reaction proceeds, yielding materials of similar overall composition and MW. These profiles are also reflected in the T_g development as the polymerization progresses. After 2.0 h, the S*grad*NBA62 aliquot sample has a T_g endset much closer to that of PS, but with increasing reaction time, T_o extends to much lower temperatures than seen with S*grad*NBA59. Consequently, the final S*grad*NBA62 sample exhibits ΔT_g = 101 °C, nearly a factor of 2 greater than that of S*grad*NBA59.

To examine the effect of MW on the T_g breadth of gradient copolymers, a lower MW sample was produced with a sigmoidal profile (S*grad*NBA73, M_n = 40 700 g/mol). The molecular and T_g characterizations of its aliquots are reported in Table 2 and Figure 3c. From the F_S vs M_n data, it can be seen that the initial addition of nBA is slower than the linear S/nBA copolymer case, consistent with a more sigmoidal profile. The T_g response of the initial aliquot resembles that of the sigmoidal S*grad*NBA62 initial aliquot, with a relatively narrow breadth. However, its development with increasing reaction time is closer to that of the linear S*grad*NBA59 case, as it maintains a peak-like shape up to 5.0 h of polymerization time, and only begins to broaden somewhat at longer reaction times. The final ΔT_g of the lower MW S*grad*NBA73 is 37.0 °C, less than the ΔT_g of both higher MW gradient cases. However, comparing the final sample to a partial gradient copolymer with similar F_S and

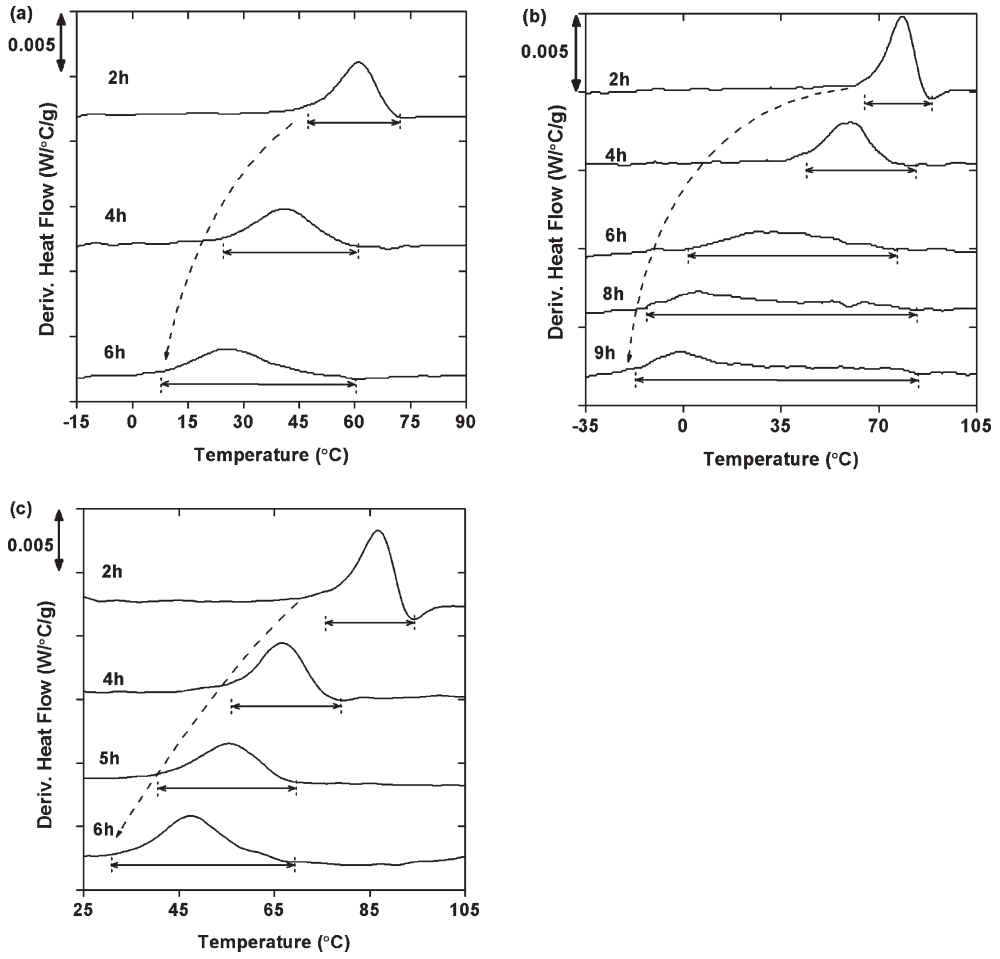

Figure 3. Derivatives[76] of DSC heating curves for aliquots and final products of (a) S*grad*NBA59, (b) S*grad*NBA62, and (c) S*grad*NBA73.

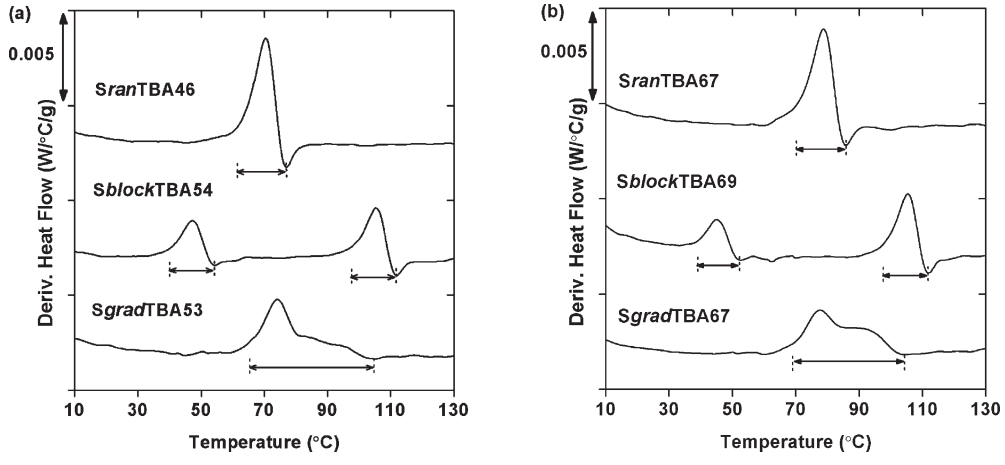

Figure 4. Derivatives[76] of DSC heating curves for S/tBA copolymers with (a) F_S = 0.46−0.54 and (b) F_S = 0.67−0.69.

M_n (S*grad*NBA59 2.0 h aliquot), we see that ΔT_g of S*grad*NBA73 is 10 °C broader, likely due to the shift to stronger phase separation with a more sigmoidal profile. Thus, in accord with theory,[40,41] both gradient profile and MW are effective in controlling the level (composition profile amplitude) of nanophase separation in moderately segregating gradient copolymers.

B.2. S/tBA Copolymers. Copolymers of S/tBA were synthesized and characterized to provide a system with similar segregation strength to S/nBA but closer homopolymer T_gs. Since tBA and nBA are isomers, their χ values are expected to be similar,[47,48,51] leading to comparable degrees of ordering in S/tBA and S/nBA gradient copolymers. The derivatives of DSC heating curves for compositionally symmetric (F_S = 0.46−0.54) S/tBA copolymers are shown in Figure 4a; those of copolymers with higher F_S values (F_S = 0.67−0.69) are shown in Figure 4b. The corresponding molecular and T_g characterizations are reported in Table 1.

Regardless of their F_S values, the diblock and random S/tBA copolymers yield narrow T_g breadths of 15−17 °C. In contrast, S*grad*TBA53 and S*grad*TBA67 exhibit ΔT_gs of 35−40 °C, indicating significant heterogeneity. The resulting

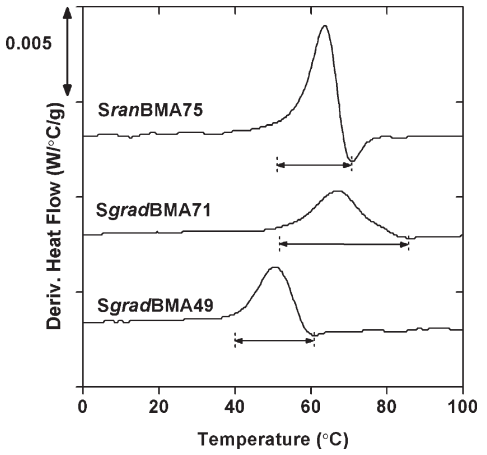

Figure 5. Derivatives[76] of DSC heating curves for S/BMA copolymers.

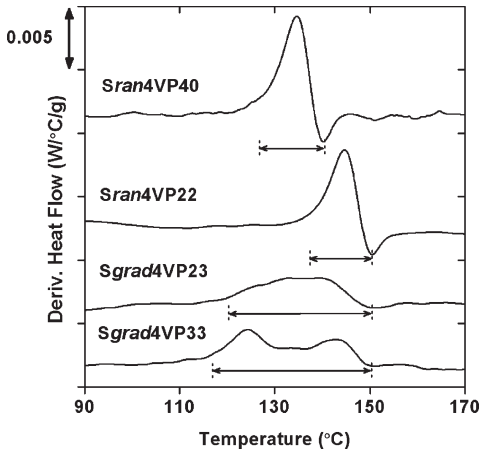

Figure 6. Derivatives[76] of DSC heating curves for S/4VP copolymers.

ΔT_g values of S/tBA gradient copolymers are noticeably smaller than those of S/nBA gradient copolymers due to the reduced T_g difference between PS and PtBA homopolymers (~60 °C) compared to that of PS and PnBA (~150 °C). It should also be noted that, similar to S/nBA gradient copolymers, the T_o and T_e values of S/tBA gradient copolymers do not fully extend to the T_g values of PtBA and PS homopolymers. Both S/tBA gradient samples were synthesized using constant tBA addition, so the combination of a linear gradient profile and moderate segregation strength likely generated sinusoidal profiles with moderate amplitude, similar to the S/nBA linear case.

B.3. S/BMA Copolymers. Previous studies on diblock copolymers have shown that S/BMA is a very weakly segregating system.[55,56,77] In particular, given the reported values of χ ranging from 0.012−0.015[55] to 0.017−0.018,[56] one would expect that symmetric S/BMA diblock copolymers should require M_n values approaching or exceeding ~100 000 g/mol to exhibit significant signatures of ordering. Correspondingly, for S/BMA gradient copolymers with M_n values below 100 000 g/mol, we would expect the overall T_g breadth would exhibit at most small differences in ΔT_g values as compared with random copolymers. To investigate this, a random copolymer (S*ran*BMA75, prepared at 70 °C), a moderately high MW gradient copolymer (S*grad*BMA71), and a low MW gradient copolymer (S*grad*BMA49), all with apparent M_n below 100 000 g/mol, were synthesized and characterized by DSC (see Figure 5 and Table 1).

Similar to S/nBA and S/tBA random copolymers, the 20 °C ΔT_g of S*ran*BMA75 indicates a lack of nanoscopic heterogeneity. The ΔT_g of the lower MW gradient copolymer (S*grad*BMA49, M_n = 57 800 g/mol), is only 21 °C, almost identical to that of S*ran*BMA75, and indicative of a disordered microstructure in S*grad*BMA49 due to low segregation strength. For the higher MW gradient copolymer (S*grad*BMA71, M_n = 83 000 g/mol), ΔT_g = 33.7 °C. For comparison, the T_g breadth of S*grad*TBA67 (a sample with similar overall MW and composition) is 42.5 °C, about 9 °C broader, even though the T_g difference between PBMA and PS is larger (~80 °C[49]) than that of PtBA and PS (~60 °C[49]). This indicates the crucial role of segregation strength (χ value) in determining the overall T_g breadth of gradient copolymers.

B.4. S/4VP Copolymers. The S/4VP system is one of two strongly segregating systems studied here (see Figure 6 and Table 3). Two random copolymers (F_S = 0.22 and 0.40) and two gradient copolymers (F_S = 0.23 and 0.33) were prepared and analyzed by DSC. The S/4VP random copolymers exhibited small ΔT_gs, ~12 °C. In contrast, the S/4VP gradient copolymers exhibited ΔT_g = 32−35 °C, spanning most of the range between the PS and P4VP homopolymer T_gs (~40 °C) and larger in magnitude than the ΔT_g obtained with the weakly segregating S/BMA blocky gradient copolymer (where there is an ~80 °C difference in PS and PBMA homopolymer T_gs). This indicates that the high χ parameter for the S/4VP system led to large amplitudes of the composition profiles in the nanophase segregated gradient copolymers.

B.5. S/AS Copolymers. The S/AS system is the second strongly segregating system addressed here. Previously, we published DSC results for S/AS block, random, and two high MW gradient copolymers.[31] The gradient copolymers exhibited ΔT_g = ~25 °C, spanning nearly the full range of temperatures between the PS and PAS T_gs. While ΔT_g was limited due to the proximity of the homopolymer T_gs, the derivative curves showed significant contributions from a range of compositions rather than the sharp peak observed in the random copolymer.

Here, we report on the ΔT_g development of a lower molecular weight S/AS gradient copolymer through DSC analysis of aliquots of partial gradient materials formed during the reaction (Table 4 and Figure 7a). The polymerization started from S monomer, and AS was added at a constant rate throughout the reaction to create a linear profile. After 2.0 h of reaction, the T_g response appears as a narrow peak near the T_g transition of pure PS. At 3.0 h of reaction, the partial gradient copolymer phase segregates to span a range of compositions, as the top of the DSC derivative peak broadens into a near plateau, reflecting a summation of multiple compositions. This is markedly different from the much higher molecular weight S/nBA linear gradient case (S*grad*NBA59), where even at 4.0 h the shape of the curve remains peak-like. This suggests that the composition profile in the S/nBA system initially evolves as a "moving average" with minimal local heterogeneity at low molecular weights, when χN is presumably less than or close to $(\chi N)_c$. The S/BMA final gradient cases also exhibit such peak-like shapes. In contrast, with S/AS, the much higher χ value pushes the system above the separation threshold, anchoring the composition profiles to the starting compositions and causing the spread. This spread continues through 5.0 h of reaction with a final ΔT_g = 22 °C. Similar plateau-like growth was observed in the ΔT_g development of S/4VP gradient copolymer aliquots (not shown).

A series of S/AS blocky random copolymers[35] of similar MW were also studied. These copolymers were synthesized

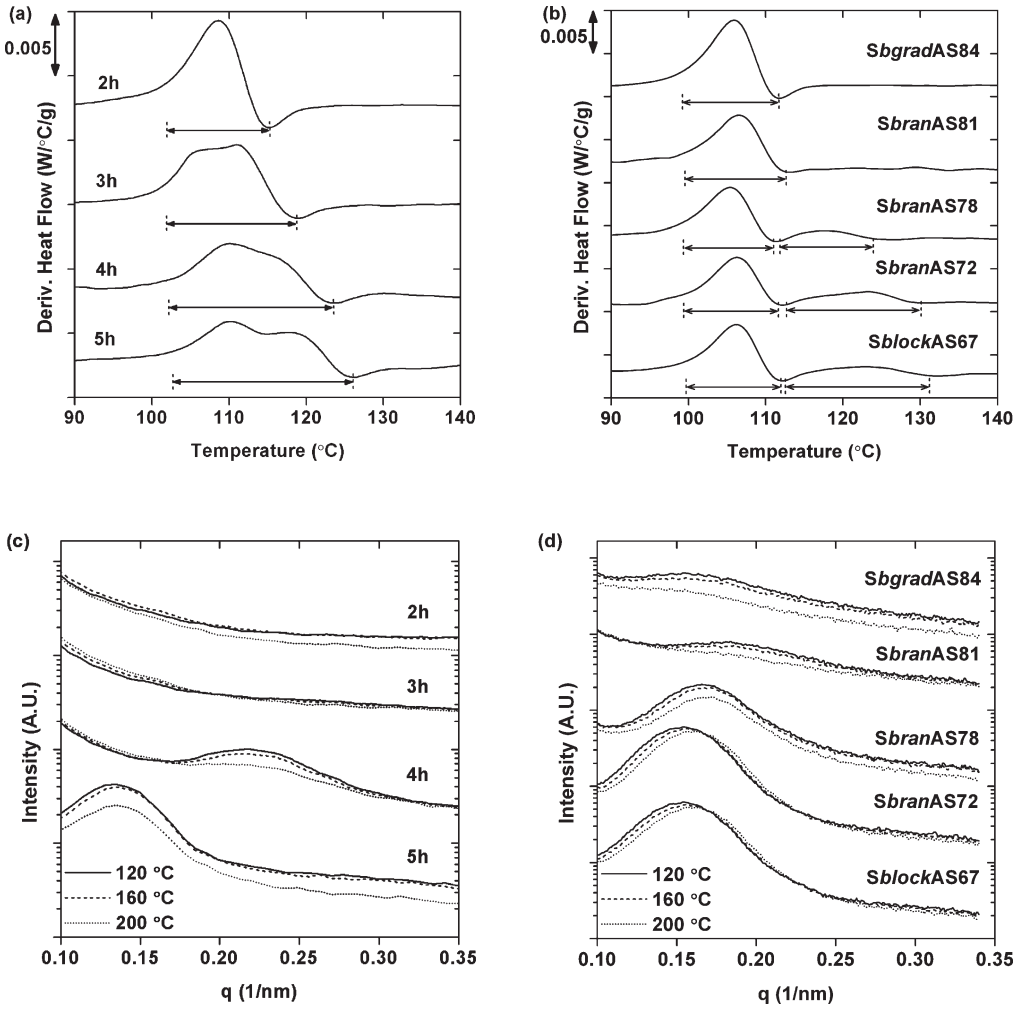

Figure 7. Derivatives[76] of DSC heating curves for (a) aliquots and final product of S*grad*AS64 and (b) S/AS blocky gradient, blocky random, and diblock copolymers. Small-angle X-ray scattering at 120, 160, and 200 °C for (c) aliquots and final product of S*grad*AS64 and (d) S/AS blocky gradient, blocky random, and diblock copolymers.

by chain extending an S/AS random block from a pure S block. The random block composition was varied through the molar ratio of S:AS monomer in the reaction mixture: 75:25 for S*bran*AS81, 50:50 for S*bran*AS78, and 25:75 for S*bran*AS72. This allowed control over the incompatibility or effective χ between the two blocks, thereby tuning the amplitude of the composition profile of the phase segregated materials. In addition, S/AS diblock (S*block*AS67) and blocky gradient (S*bgrad*AS84) cases were synthesized, the latter by slowly increasing the amount of AS in a chain extension mixture.

Figure 7b shows the DSC derivative curves of the blocky gradient, blocky random, and diblock copolymers. The two copolymers with the lowest AS incorporations, S*bran*AS81 and S*bgrad*AS84, show only subtle T_g broadening, indicating that they are weakly segregated. The others (S*bran*AS78, S*bran*AS72, S*block*AS67) show well-separated peaks indicating strong phase segregation, in contrast with the S/AS partial and full gradient copolymers (Figure 7a).

To complement the thermal analysis, SAXS analysis was used to investigate further the level and strength of phase segregation achieved in S/AS gradient copolymers compared to those achieved by blocky random and blocky gradient copolymers. Scattering profiles were taken at 120, 160, and 200 °C. The level and range of composition change achieved in the phase-segregated materials can be interpreted from the relative intensity of the peaks, while the strength of the segregation can be seen from the change in intensity with respect to temperature.

The SAXS results for the S/AS gradient copolymer aliquots are shown in Figure 7c. No peak is observed for the 2.0 h case; no phase segregation was expected in this case since it had exhibited a narrow T_g peak. In the 3.0 h case, which exhibited a slightly broadened, plateau-like T_g response, there appears to be very subtle evidence of scattering at $q \sim 0.25-0.30$ at the lowest temperature; it is possible that this sample had only a low amplitude of variation in its composition profile, resulting in insufficient contrast between phase-separated regions to yield substantial scattering. For the 4.0 h sample, a small peak is observed which diminishes with increasing temperature. In the final material (5.0 h), a strong peak is seen at a lower q value, consistent with increasing MW and gradient development.

The SAXS results for the blocky random and blocky gradient copolymers are shown in Figure 7d. Signatures of phase segregation are seen for even S*bran*AS81 and S*bgrad*AS84, which have low AS content. These two materials reveal similar low levels of phase segregation, with the weak scattering peak nearly disappearing at 200 °C. The S*bran*AS78 sample exhibits a stronger peak which diminishes only slightly at 200 °C, and the S*bran*AS72 and pure diblock samples show strong peaks which change little in intensity with temperature. The peak maxima shift to lower q values with increasing AS levels, despite similarity in MWs.

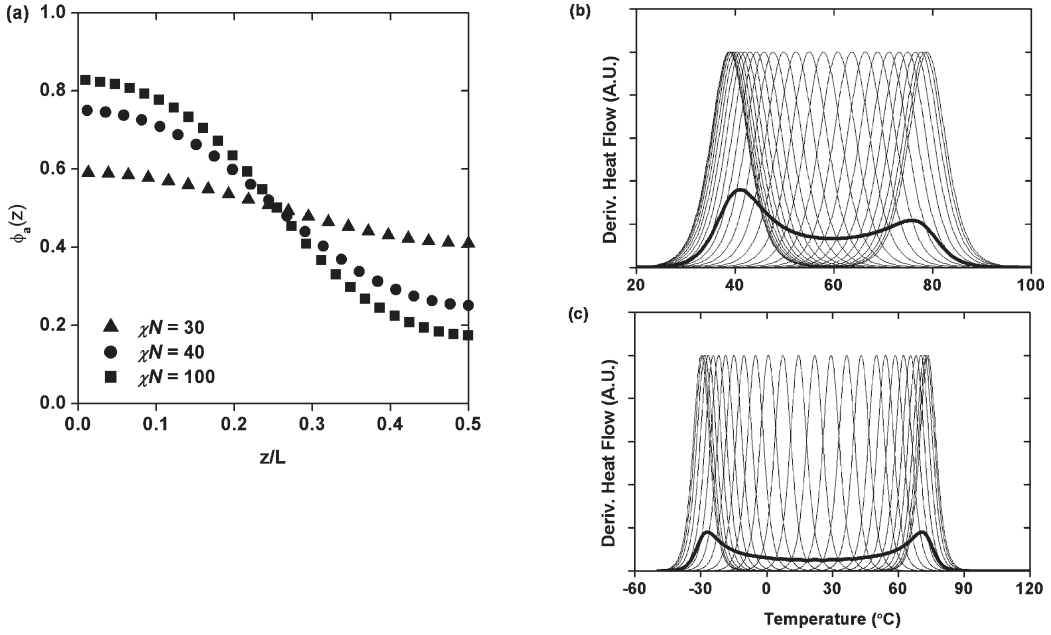

Figure 8. (a) Equilibrium lamellar compositions for a symmetric linear gradient copolymer calculated at $\chi N = 30, 40$, and 100 using SCMF techniques. The period of the lamellar structure is L. Predicted DSC derivative heat flow curves for (b) S/BMA and (c) S/nBA linear gradient copolymers with $\chi N = 100$. The thin lines are the derivative heat flow traces corresponding to copolymers with the composition fractions predicted in the composition profile, while the bold line is the area-normalized summation of the individual composition fraction traces. (Note: material-specific heat capacities were not accounted for in these predictions.)

This may result from stretched conformations of the more phase segregated blocky random cases.

A comparison of the 4.0 h aliquot with the blocky random cases reveals SAXS behavior most similar to that of S*bran*AS81. However, while the MWs are similar, the incorporation of AS into the gradient aliquot is much higher than in S*bran*AS81 and is closer to levels in the pure diblock cases and S*bran*AS72. Thus, a gradient structure can increase compatibility beyond the comonomer mixing achieved with a blocky random structure. Overall, the level of scattering seen in the 5.0 h sample is between those in S*bran*AS78 and S*bran*AS72, indicating that a similar level of phase segregation can be achieved using gradient structures or random blocks.[78]

C. Predictions of Glass Transition Breadth. To verify the relationship between the observed T_g breadths and the level of nanophase separation expected for the various copolymer systems, we compare our experimental results against those predicted by theory for gradient copolymer nanophase separation. In order to calculate the predicted T_g breadths, experimental results from the sets of random copolymers were used to determine the composition dependence of T_g for each copolymer system. (It should be noted that random copolymers prepared by ContRP yielded similar T_g breadths and values as random copolymers made by ConvRP [Supporting Information]). The S/tBA, S/nBA, S/AS, and S/4VP systems were well described by straight-line fits of T_g as a function of F_S while the S/BMA system was weighted toward the T_g of PBMA and was best fit using a Gordon−Taylor equation (for specific T_g composition data please see the Supporting Information):[56,63,79,80]

$$T_{g,\,S/nBA} = 157F_S + 218 \quad (1)$$

$$T_{g,\,S/tBA} = 58F_S + 321 \quad (2)$$

$$T_{g,\,S/AS} = -21F_S + 404 \quad (3)$$

$$T_{g,\,S/4VP} = -46F_S + 424 \quad (4)$$

$$T_{g,\,S/BMA} = (107F_S + 921F_{BMA})/(F_S + 3F_{BMA}) \quad (5)$$

From eqs 1−5 (with T_g [=] K) and composition profiles generated by the SCMF method, plots of derivative heat flow can be created for a given comonomer distribution. The equilibrium lamellar composition profiles consist of discrete points representing a set of compositions distributed over equal volume fractions (e.g., see Figure 8a). Each of these volume fractions is assumed to contribute a glass transition response corresponding to its unique composition. Since tanh functions have been used in the past for fitting DSC heat flow data,[81] a tanh function derivative was used to represent these individual contributions to the derivative heat flow curves:

$$y = 1 - (\tanh((T - T_{peak})/5))^2 \quad (6)$$

where y is the peak-normalized derivative heat flow value given as a function of temperature (T). The appearance of the tanh function derivative is a sharp, symmetric peak, similar to the derivative heat flow curves of homopolymers and random copolymers. For each of these individual contributions, the peak location (T_{peak}) was determined from the predicted volume fraction composition and one of eqs 1−5, while a peak breadth of ~17 °C (measured at the baseline) was used, since most of our random copolymers exhibited breadths of 15−20 °C. The tanh function derivatives representing all the individual volume fractions were then summed to give the predicted glass transition response for the material as a whole (e.g., Figure 8b,c). The final plotted response was normalized by the area under the curve.

To demonstrate the manner in which the gradient copolymer T_g breadths increase with respect to χN, predicted derivative heat flow curves are shown for a symmetric, linear gradient copolymer of each copolymer system at $\chi N = 30$,

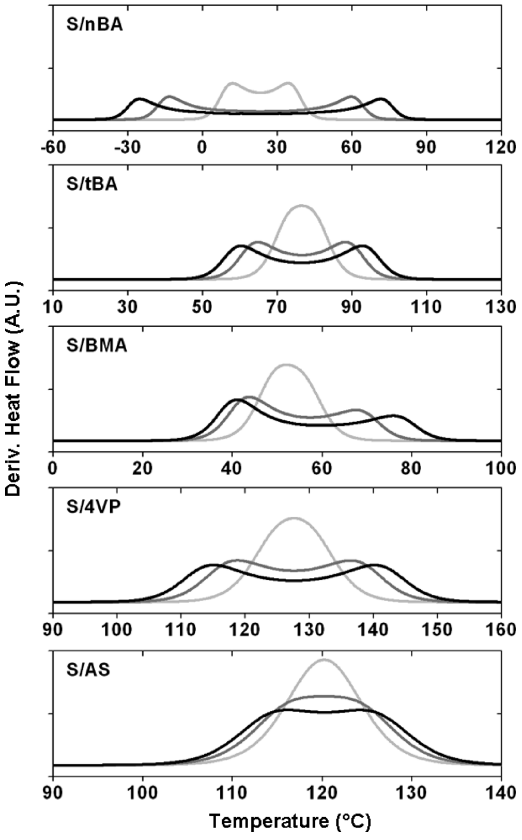

Figure 9. Predicted DSC derivative heat flow curves for S/nBA, S/tBA, S/BMA, S/4VP, and S/AS symmetric linear gradient copolymers with $\chi N = 30$ (light gray), $\chi N = 40$ (dark gray), and $\chi N = 100$ (black).

40, and 100 (Figure 9). Since the composition dependence of T_g for the S/nBA, S/tBA, S/4VP, and S/AS systems follow a linear relationship, their derivative heat flow curves appear symmetric, while the S/BMA curves are asymmetric as a result of their Gordon−Taylor equation-based relationship. The local peaks seen at the higher and lower temperature extremes in the predicted curves derive from the higher fraction of material at the peaks and troughs of the sinusoidal composition profiles, and similar local peaks are seen in a number of our experimental materials.

The $\chi N = 30$ cases just exceed the predicted critical χN parameter of 29.25[40] or 29.55[41] for this architecture; thus, the level of phase separation is quite low (amplitude = 0.2), and the T_g breadths are correspondingly narrow. The level of phase separation increases with increasing χN, with the amplitude increasing to 0.5 for $\chi N = 40$ and to 0.7 for $\chi N = 100$. The T_g breadths increase accordingly, and curves which had appeared monomodal at $\chi N = 30$ develop more multimodal appearances. This reflects the discussion above of plateau-like vs peak-like curves seen experimentally for materials of differing levels of phase separation. The magnitudes of the calculated breadths reflect what we had observed experimentally except for the S/BMA system; this reinforces our conclusion that the S/BMA gradient materials are phase-mixed. Similar to our experimental observations, the breadth change predicted for the S/AS system is small, as a result of the relatively close T_g values of the homopolymers; in contrast, the S/nBA system is predicted to demonstrate a substantial change because of the extreme difference between the T_gs of PS and PnBA.

As a final point of comparison, composition profiles were generated reflecting the compositions, molecular weights, and architectures of our experimental block and gradient copolymer materials. The architectures were simplified as either linear functions or tanh functions depending on the rate of second monomer addition during the sample preparation, and the details of the functions were adjusted to yield the expected compositions for the final chain lengths (see Supporting Information for equations). The construction of the aliquot cases was based on the function used for the final polymer material but cut off at a point reflecting the aliquot molecular weight. In the case of S/nBA and S/BMA, where different Flory−Huggins parameters were found in the literature, both the highest and lowest values were used to calculate upper and lower bounds on the phase segregation. The calculated derivative T_g curves are shown in Figure 10. The S/BMA and some S/nBA aliquot results are not shown as they were found to be phase mixed over all Flory−Huggins parameters. Since there was no MW characterization of the S/4VP materials, this analysis method was not applied to that system.

The S/nBA gradient samples and aliquots that exhibited phase separation also demonstrate a very strong phase separation dependence on χ. Comparing the calculated T_g breadths against those measured experimentally, it appears that S/nBA may possess a Flory−Huggins interaction parameter intermediate to those implemented in the calculations. The lower value ($\chi = 0.034$) predicts that the linear gradient (S*grad*NBA59) and the 6 h increasing gradient aliquot (S*grad*NBA62-6h) remain below the critical point of separation, whereas the experimental T_g breadths indicate some degree of phase segregation. Meanwhile, application of the higher value ($\chi = 0.087$) overpredicts the T_g breadths by a significant amount. The block copolymer, being in the strongly phase segregating regime, shows less dependence on χ. These results indicate that, in addition to verification of experimental results, using SCMF to predict T_g breadths provides a novel means of checking on reported values of χ parameters. To test this, calculations were performed on the S/nBA cases using χ values intermediate to 0.034 and 0.087 at intervals of 0.005, and it was found that $\chi = 0.055$ gave T_g breadths most consistent with the experimental results. The T_g breadth for the linear gradient case (S*grad*NBA59) was calculated as 47 °C compared to the experimental value of 53.9 °C, while that for S*grad*NBA62 was calculated as 113 °C compared to the experimental value of 101.2 °C. Additionally, ΔT_g was predicted to increase by 18 °C between S*grad*NBA62-6h and the final material at 9 h, while experimentally the ΔT_g change was 20 °C. Given the large shifts in T_g that occur between S/nBA copolymers of different compositions, these values are in excellent accord.

A point to note is that while we have not included magnitude of heat capacity change with respect to composition as part of our treatment of the data, this would be an important variable for future study, since it contributes to determining the overall shape of the derivative heat flow curves. For example, the S*block*NBA46 experimental data show a significantly greater glass transition peak for PnBA than PS, despite the near symmetry in composition of the system. An inherently lower heat capacity signal for higher styrene content regions in the S/nBA gradient copolymers would explain the lack of local peaks at the higher temperature ends of their experimental T_g breadth data, as compared to the calculated curves.

The calculated derivative heat flow curves for the S/tBA block copolymers closely resemble those from experiment. The two gradient cases are less close; the S*grad*TBA53 case is overpredicted while the S*grad*TBA67 case is underpredicted. This outcome suggests that our assumption of strictly linear gradient architectures may be oversimplified. More accurate

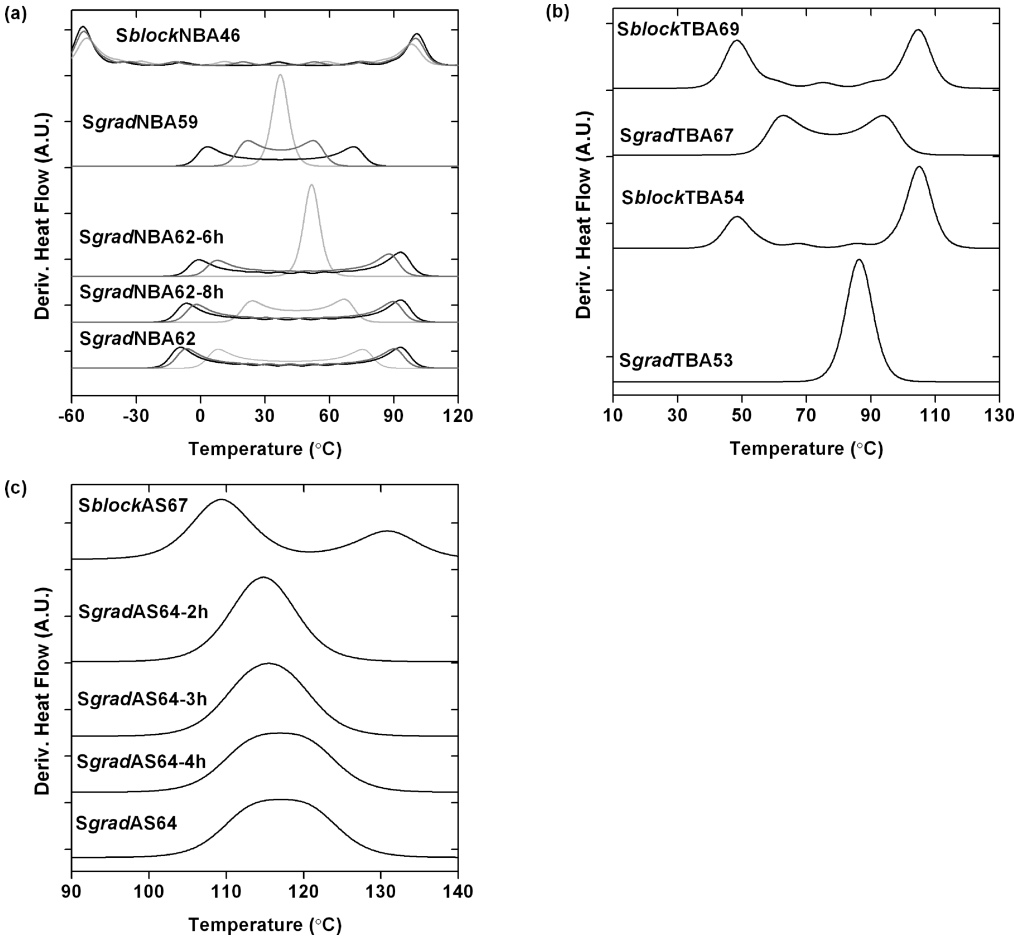

Figure 10. Predicted DSC derivative heat flow curves for (a) S/nBA copolymers (calculated using $\chi = 0.034$ (light gray), $\chi = 0.055$ (dark gray), and $\chi = 0.087$ (black)), (b) S/tBA copolymers, and (c) S/AS copolymers.

representations of the chain structures could potentially be created by computer modeling and programmed synthesis[22,82] reflecting reaction conditions, addition rates, and reactivity ratios.

Finally, the calculated S/AS cases resemble what was measured experimentally, with an initially monomodal peak extending to higher temperatures with increasing reaction time to create a slightly broader, more plateau-like shape. The predicted T_g breadth increases from $\Delta T_g \sim 17$ °C at 2 h of reaction to $\Delta T_g \sim 25$ °C after 5 h of reaction, consistent with the observed experimental change of ΔT_g from 14.0 to 21.5 °C. The somewhat greater breadths seen from the calculations could arise from the assumption of a 17 °C breadth for the tanh derivative function, which slightly overpredicts the breadths for this copolymer system.

D. Origin and Implications of the Broad Glass Transition in Gradient Copolymers. Polymer systems exhibiting breadth in T_g response include some miscible blends and disordered block copolymers,[50,69,70] athermal blends of a polymer and its oligomer,[83] (multi)block copolymers with broad interfacial width,[50,71,72] and nanoconfined systems.[74,75,84] Our previous studies on strongly segregating S/HS and S/AA gradient copolymers revealed the presence of substantial T_g breadths,[31,33] with the S/HS system exhibiting unusually large T_g breadth ($\Delta T_g = \sim 80$ °C) in comparison with other heterogeneous polymeric materials. The present study has expanded the focus to include copolymers with a wide range of segregation strengths and gradient architectures. The two strongly segregating S/AS and S/4VP systems demonstrated behavior similar to the S/HS case, with ΔT_g spanning 70−80% of the homopolymer T_g difference. However, the moderately segregating S/nBA and S/tBA systems and the very weakly segregating S/BMA system show not only significantly reduced ΔT_gs relative to the homopolymer T_g differences, but, in the case of moderately segregating systems, also a significant influence of gradient architecture on the ΔT_g breadth. In particular, it is important to note that, as shown in the present study, appropriate design of the gradient copolymer composition profile can lead to T_g breadth that exceeds 100 °C (> 65% of the homopolymer T_g difference) even in moderately segregating systems, e.g., S*grad*NBA62 with $\Delta T_g = 101.2$ °C.

In gradient copolymer melts, the smoothly varying comonomer sequences along the chain length combined with the comonomer repulsive interactions lead to the formation of an ordered microphase, where the local composition profile within the nanophase is a continuous, sinusoidal function across the unit cell.[40,41] Upon heating from the glassy state, the glass transition associated with each composition present across the nanodomains is expressed, resulting in a net broadening of T_g responses in comparison with random copolymers. Accordingly, the T_g breadth in a gradient copolymer is influenced by two main factors: the χN of the system relative to $(\chi N)_c$ and the inherent difference in cooperative segmental mobility between the comonomers (homopolymer T_g difference). As in block copolymers, the χN of the system itself can be controlled through MW (proportional to N) and the inherent comonomer incompatibility (χ). With gradient copolymers, the additional factor available for tuning is the gradient profile, which directly

affects $(\chi N)_c$.[40,41] (Recall that $(\chi N)_c$ shifts from 29.25 to 29.55 for a fully linear gradient copolymer[40,41] to 10.495 for a symmetric diblock copolymer.[45]) In a more block-like or sigmoidal gradient copolymer, the system will have a lower $(\chi N)_c$[41] and thus be further removed from the weak segregation limit than a linear gradient copolymer of the same MW. This results in a continuously varying composition profile with greater amplitude and a higher ΔT_g.

For comonomer systems with very high χ values, we expect gradient copolymers to yield χN values that substantially exceed $(\chi N)_c$ even at moderate MWs and gradient profiles, with the result that ΔT_g spans most of the difference in homopolymer T_g. When the difference in cooperative segmental mobility of comonomers (and hence difference in T_g values of the respective homopolymers) is substantial, as in S/HS systems, gradient copolymers may exhibit very large T_g breadths (e.g., $\Delta T_g = \sim 80$ °C in S/HS gradient copolymers[31]). When the inherent difference in cooperative segmental mobility is small, e.g., in S/AS and S/4VP systems, gradient copolymers will be phase segregated (as seen by SAXS), but ΔT_g will be relatively small.

For systems with moderate χ values, such as S/nBA or S/tBA copolymers, the overall χN values of gradient copolymers are expected to be closer to $(\chi N)_c$; thus, the ΔT_gs of such gradient copolymers are highly sensitive to gradient design and MW. For example, in the comparison of S*grad*NBA59 and S*grad*NBA62, a shift from a more linear profile to a more sigmoidal profile almost doubles ΔT_g from 54 to 101 °C. However, as seen by comparison of S*grad*NBA62 to S*grad*NBA73, creating a polymer with a similar sigmoidal profile but half the MW reduces ΔT_g to 37 °C. When a system has an extremely small χ value, as in the S/BMA system, the gradient copolymer exhibits a ΔT_g comparable to or only slightly larger than that of a random copolymer. This suggests that even with high MWs, χN for this system remains below $(\chi N)_c$.

Our study shows that the level of compositional heterogeneity of nanophase-separated gradient copolymers can be highly tuned and that this consequently acts as an exquisite means for controlling the glass transition response. Basic DSC measurements and application of the derivative analysis method[76] can serve as a rapid and simple means for qualitative evaluation of gradient copolymer nanophase separation. Quantitative or semiquantitative evaluation of the composition profiles present in nanophase-separated gradient copolymers may be achieved by comparison of the experimentally determined T_g breadths to those determined from composition profiles calculated via SCMF techniques. Knowledge of this type has broad implications as the nanophase structures of copolymers can have substantial influence on a broad array of mechanical behavior including deformation mechanisms[55,85] and damping properties.[34,86,87]

Acknowledgment. We acknowledge the support of the NSF-MRSEC program (Grant DMR-0520513), Northwestern University, the Brain Korea 21 program, a 3M fellowship (J.K.), and an Intel Fellowship (M.M.M.). We thank Soyoung Kim and Golnar Doroudian for their contributions in synthesis and Arkema for a generous donation of BlocBuilder. Parts of this work were carried out in the Institute of Technology Characterization Facility, University of Minnesota, which is a member of the NSF-funded Materials Research Facilities Network (www.mrfn.org).

Supporting Information Available: Reported reactivity ratios of S/nBA, S/tBA, S/4VP, S/AS, and S/BMA copolymer systems (Table 1); random copolymers of S/nBA, S/tBA, S/4VP, and S/AS prepared using conventional radical polymerization (Table 2); random S/BMA copolymer materials (Table 3); random copolymers of S/nBA, S/tBA, S/4VP, and S/AS prepared using ConvRP vs ContRP (Table 4); summary of reaction conditions and polydispersities for polymers (Table 5); summary of molecular characterization for S/nBA, S/tBA, S/BMA, S/4VP, and S/AS gradient copolymer aliquots (Table 6); summary of equations representing experimental gradient copolymer architectures used in SCMF calculations (Table 7). This material is available free of charge via the Internet at http://pubs.acs.org.

References and Notes

(1) Georges, M. K.; Veregin, R. P. N.; Kazmaier, P. M.; Hamer, G. K. *Macromolecules* **1993**, *26*, 2987–2988.
(2) Wang, J. S.; Matyjaszewski, K. *J. Am. Chem. Soc.* **1995**, *117*, 5614–5615.
(3) Chiefari, J.; Chong, Y. K.; Ercole, F.; Krstina, J.; Jeffery, J.; Le, T. P. T.; Mayadunne, R. T. A.; Meijs, G. F.; Moad, C. L.; Moad, G.; Rizzardo, E.; Thang, S. H. *Macromolecules* **1998**, *31*, 5559–5562.
(4) Hawker, C. J.; Bosman, A. W.; Harth, E. *Chem. Rev.* **2001**, *101*, 3661–3688.
(5) Matyjaszewski, K. *Controlled/Living Radical Polymerization from Synthesis to Materials*; American Chemical Society: Washington, DC, 2006; Vol. *944*.
(6) Benoit, D.; Chaplinski, V.; Braslau, R.; Hawker, C. J. *J. Am. Chem. Soc.* **1999**, *121*, 3904–3920.
(7) Mok, M. M.; Pujari, S.; Burghardt, W. R.; Dettmer, C. M.; Nguyen, S. T.; Ellison, C. J.; Torkelson, J. M. *Macromolecules* **2008**, *41*, 5818–5829.
(8) Beginn, U. *Colloid Polym. Sci.* **2008**, *286*, 1465–1474.
(9) Zaremski, M. Y.; Kalugin, D. I.; Golubev, V. B. *J. Polym. Sci., Ser. A* **2009**, *51*, 103–122.
(10) Matyjaszewski, K.; Ziegler, M. J.; Arehart, S. V.; Greszta, D.; Pakula, T. *J. Phys. Org. Chem.* **2000**, *13*, 775–786.
(11) Davis, K. A.; Matyjaszewski, K. *Adv. Polym. Sci.* **2002**, *159*, 1–169.
(12) Buzin, A. I.; Pyda, M.; Costanzo, P.; Matyjaszewski, K.; Wunderlich, B. *Polymer* **2002**, *43*, 5563–5569.
(13) Qin, S. H.; Saget, J.; Pyun, J. R.; Jia, S. J.; Kowalewski, T.; Matyjaszewski, K. *Macromolecules* **2003**, *36*, 8969–8977.
(14) Mignard, E.; Leblanc, T.; Bertin, D.; Guerret, O.; Reed, W. F. *Macromolecules* **2004**, *37*, 966–975.
(15) Inoue, Y.; Watanabe, J.; Takai, M.; Yusa, S.; Ishihara, K. *J. Polym. Sci., Part A: Polym. Chem.* **2005**, *43*, 6073–6083.
(16) Neugebauer, D.; Zhang, Y.; Pakula, T. *J. Polym. Sci., Part A: Polym. Chem.* **2006**, *44*, 1347–1356.
(17) Paris, R.; De la Fuente, J. L. *J. Polym. Sci., Part B: Polym. Phys.* **2007**, *45*, 1845–1855.
(18) Karaky, K.; Péré, E.; Pouchan, C.; Desbrières, J.; Dérail, C.; Billon, L. *Soft Matter* **2006**, *2*, 770–778.
(19) Karaky, K.; Billon, L.; Pouchan, C.; Desbrières, J. *Macromolecules* **2007**, *40*, 458–464.
(20) Karaky, K.; Dérail, C.; Reiter, G.; Billon, L. *Macromol. Symp.* **2008**, *267*, 31–40.
(21) Jouenne, S.; González-Léon, J. A.; Ruzette, A.-V.; Lodefier, P.; Tencé-Girault, S.; Leibler, L. *Macromolecules* **2007**, *40*, 2432–2442.
(22) Sun, X. Y.; Luo, Y. W.; Wang, R.; Li, B. G.; Zhu, S. P. *AIChE J.* **2008**, *54*, 1073–1087.
(23) Jakubowski, W.; Juhari, A.; Best, A.; Koynov, K.; Pakula, T.; Matyjaszewski, K. *Polymer* **2008**, *49*, 1567–1578.
(24) Cypryk, M.; Delczyk, B.; Juhari, A.; Koynov, K. *J. Polym. Sci., Part A: Polym. Chem.* **2009**, *47*, 1204–1216.
(25) Gray, M. K.; Zhou, H. Y.; Nguyen, S. T.; Torkelson, J. M. *Polymer* **2004**, *45*, 4777–4786.
(26) Gray, M. K.; Zhou, H. Y.; Nguyen, S. T.; Torkelson, J. M. *Macromolecules* **2004**, *37*, 5586–5595.
(27) Woo, D.; Kim, J.; Suh, M. H.; Zhou, H. Y.; Nguyen, S. T.; Lee, S. H.; Torkelson, J. M. *Polymer* **2006**, *47*, 3287–3291.
(28) Kim, J.; Zhou, H. Y.; Nguyen, S. T.; Torkelson, J. M. *Polymer* **2006**, *47*, 5799–5809.
(29) Kim, J.; Gray, M. K.; Zhou, H. Y.; Nguyen, S. T.; Torkelson, J. M. *Macromolecules* **2005**, *38*, 1037–1040.
(30) Tao, Y.; Kim, J.; Torkelson, J. M. *Polymer* **2006**, *47*, 6773–6781.

(31) Kim, J.; Mok, M. M.; Sandoval, R. W.; Woo, D. J.; Torkelson, J. M. *Macromolecules* **2006**, *39*, 6152–6160.
(32) Wong, C. L. H.; Kim, J.; Roth, C. B.; Torkelson, J. M. *Macromolecules* **2007**, *40*, 5631–5633.
(33) Wong, C. L. H.; Kim, J.; Torkelson, J. M. *J. Polym. Sci., Part B: Polym. Phys.* **2007**, *45*, 2842–2849.
(34) Mok, M. M.; Kim, J.; Torkelson, J. M. *J. Polym. Sci., Part B: Polym. Phys.* **2008**, *46*, 48–58.
(35) Kim, J.; Sandoval, R. W.; Dettmer, C. M.; Nguyen, S. T.; Torkelson, J. M. *Polymer* **2008**, *49*, 2686–2697.
(36) Dettmer, C. M.; Gray, M. K.; Torkelson, J. M.; Nguyen, S. T. *Macromolecules* **2004**, *37*, 5504–5512.
(37) In the strict definition of the term, "random copolymers" refer to copolymers whose distribution follows Bernoullian statistics, whereas "statistical copolymers" is the more general definition applied to distributions which are statistical. Following the conventional literature, we use the two terms interchangeably (Hiemenz, P. C.; Lodge, T. P. *Polymer Chemistry*, 2nd ed.; CRC Press: Boca Raton, FL, 2007; p 10).
(38) Pakula, T.; Matyjaszewski, K. *Macromol. Theory Simul.* **1996**, *5*, 987–1006.
(39) Aksimentiev, A.; Holyst, R. *J. Chem. Phys.* **1999**, *111*, 2329–2339.
(40) Lefebvre, M. D.; Olvera de la Cruz, M.; Shull, K. R. *Macromolecules* **2004**, *37*, 1118–1123.
(41) Jiang, R.; Jin, Q. H.; Li, B. H.; Ding, D. T.; Wickham, R. A.; Shi, A. C. *Macromolecules* **2008**, *41*, 5457–5465.
(42) Farcet, C. International Patent WO 2006003317.
(43) Lefay, C.; Charleux, B.; Save, M.; Chassenieux, C.; Guerret, O.; Magnet, S. *Polymer* **2006**, *47*, 1935–1945.
(44) Moad, G.; Dean, K.; Edmond, L.; Kukaleva, N.; Li, G. X.; Mayadunne, R. T. A.; Pfaendner, R.; Schneider, A.; Simon, G.; Wermter, H. *Macromol. Symp.* **2006**, *233*, 170–179.
(45) Leibler, L. *Macromolecules* **1980**, *13*, 1602–1617.
(46) Edgecombe, B. D.; Stein, J. A.; Frechet, J. M. J.; Xu, Z. H.; Kramer, E. J. *Macromolecules* **1998**, *31*, 1292–1304.
(47) Nicolas, J.; Ruzette, A. V.; Farcet, C.; Gérard, P.; Magnet, S.; Charleux, B. *Macromolecules* **2007**, *48*, 7029–7040.
(48) Rana, D.; Bag, K.; Bhattacharyya, S. N.; Mandal, B. M. *J. Polym. Sci., Part B: Polym. Phys.* **2000**, *38*, 369–375.
(49) Katritzky, A. R.; Sild, S.; Lobanov, V.; Karelson, M. *J. Chem. Inf. Comput. Sci.* **1998**, *38*, 300–304.
(50) Miwa, Y.; Usami, K.; Yamamoto, K.; Sakaguchi, M.; Sakai, M.; Shimada, S. *Macromolecules* **2005**, *38*, 2355–2361.
(51) The Flory−Huggins parameters for S/AS and S/tBA were calculated from group molar attraction constants after the methods of ref 51 applied to polymer systems based on theory from refs 52 and 53. A concise summary of these methods can be found in the following text: Rudin, A. In *The Elements of Polymer Science and Engineering*, 2nd ed.; Academic Press: San Diego, 1999; pp 447−458.
(52) Small, P. A. *J. Appl. Chem.* **1953**, *3*, 71.
(53) Huggins, M. L. *J. Chem. Phys.* **1941**, *9*, 440.
(54) Flory, P. J. *J. Chem. Phys.* **1941**, *9*, 660–661.
(55) Weidisch, R.; Schreyeck, G.; Ensslen, M.; Michler, G. H.; Stamm, M.; Schubert, D. W.; Budde, H.; Horing, S.; Arnold, M.; Jerome, R. *Macromolecules* **2000**, *33*, 5495–5504.
(56) Spiro, J. G.; Yang, J.; Zhang, J. X.; Winnik, M. A.; Rharbi, Y.; Vavasour, J. D.; Whitmore, M. D.; Jérôme, R. *Macromolecules* **2006**, *39*, 7055–7063.
(57) van Ekenstein, G. O. R. A.; Meyboom, R.; ten Brinke, G.; Ikkala, O. *Macromolecules* **2000**, *33*, 3752–3756.
(58) Zheng, S. X.; Mi, Y. L. *Polymer* **2003**, *44*, 1067–1074.
(59) Lessard, B.; Maric, M. *Macromolecules* **2008**, *41*, 7881–7891.
(60) Eggenhuisen, T. M.; Becer, C. R.; Fijten, M. W. M.; Eckardt, R.; Hoogenboom, R.; Schubert, U. S. *Macromolecules* **2008**, *41*, 5132–5140.
(61) Dire, C.; Belleney, J.; Nicolas, J.; Bertin, D.; Magnet, S.; Charleux, B. *J. Polym. Sci., Part A: Polym. Chem.* **2008**, *46*, 6333–6345.
(62) Gilbert, R. G.; Hess, M.; Jenkins, A. D.; Jones, R. G.; Kratochvíl, R.; Stepto, R. F. T. *Pure Appl. Chem.* **2009**, *81*, 351–353.
(63) Multiple temperatures were used for S/BMA since methacrylate materials have been known to exhibit preparation-dependent T_g values (McCrum, N. G.; Read, B. E.; Williams, G. *Anelastic and Dielectric Effects in Polymeric Solids*; John Wiley & Sons: New York, 1967; Chapter 8, pp 238−299). Temperatures were chosen to reflect those employed in the synthesis of the block and gradient copolymers. The T_g values for compositions with low styrene content show little variation with respect to polymerization type and temperature, while greater variation is seen at mid to high styrene content compositions.
(64) Shull, K. R.; Kramer, E. J. *Macromolecules* **1990**, *23*, 4769–4779.
(65) Shull, K. R. *Macromolecules* **1992**, *25*, 2122–2133.
(66) We note that it is not possible for us to prepare quantitatively accurate data showing the dependence of instantaneous styrene mole fraction incorporated in the gradient copolymers as a function of copolymer chain length as was done in: Lefebvre, M. D.; Dettmer, C. M.; McSwain, R. L.; Xu, C.; Davila, J. R.; Composto, R. J.; Nguyen, S. T.; Shull, K. R. *Macromolecules* **2005**, *38*, 10494 and ref 10. This arises from two factors. First, in Lefebvre et al. and ref 10, the instantaneous styrene mole fractions incorporated in the copolymers were determined using an equation that accounts for the change in composition in the comonomer mixture as a function of conversion. In Lefebvre et al., the comonomer mixture composition was determined by gas chromatography of the aliquots, and large changes in conversion accompanied the copolymerization. In contrast, in each of our copolymerizations, overall conversion of monomer was relatively small. Thus, we chose a different method to determine F_S values that involved recovering the copolymer from each aliquot and determining the copolymer composition using an appropriate method such as ^{1}H NMR. However, because the normalized chain length of the copolymer recovered from each of our aliquot samples is only apparent and not absolute (using M_n values obtained from GPC relative to PS standards rather than absolute values), a quantitatively accurate determination cannot be made of the instantaneous styrene mole fraction along the gradient copolymer chains.
(67) Shen, S.; Torkelson, J. M. *Macromolecules* **1992**, *25*, 721–728.
(68) Chen, X. Y.; Jankova, K.; Kops, J.; Batsberg, W. *J. Polym. Sci., Part A: Polym. Chem.* **1999**, *37*, 627–633.
(69) Agari, Y.; Shimada, M.; Ueda, A.; Nagai, S. *Macromol. Chem. Phys.* **1996**, *197*, 2017–2033.
(70) Sircar, A. K.; Galaska, M. L.; Chartoff, R. P. *J. Therm. Anal.* **1997**, *49*, 407–415.
(71) Lodge, T. P.; Wood, E. R.; Haley, J. C. *J. Polym. Sci., Part B: Polym. Phys.* **2006**, *44*, 756–763.
(72) Hourston, D. J.; Song, M.; Hammiche, A.; Pollock, H. M.; Reading, M. *Polymer* **1997**, *38*, 1–7.
(73) Masson, J. F.; Bundalo-Perc, S.; Delgado, A. *J. Polym. Sci., Part B: Polym. Phys.* **2005**, *43*, 276–279.
(74) Zhang, B.; Blum, F. D. *Macromolecules* **2003**, *36*, 8522–8527.
(75) Kabomo, M. T.; Blum, F. D.; Kulktratiyut, S.; Kulkeratiyut, S.; Krisanangkura, P. *J. Polym. Sci., Part B: Polym. Phys.* **2008**, *46*, 649–658.
(76) In using numerical derivative functions, the size of the interval over which the derivative is taken can impact the final T_g breadth. In this paper, we use a temperature range of ∼6.0−7.5 °C, consistent with our previous use the derivative technique (ref 31). At this range, we can achieve some level of noise suppression with minimal impact on the T_g breadth. We suggest using polystyrene as a control material in implementing this technique, as its T_g breadth and value are essentially independent of polymerization technique.
(77) Russell, T. P.; Karis, T. E.; Gallot, Y.; Mayes, A. M. *Nature* **1994**, *368*, 729–731.
(78) It is interesting to note that the q value of the scattering peak is lower in the gradient case than the blocky random cases, indicative of a larger period for the ordered structure in the (5.0 h) gradient copolymer. Theory predicts that the period associated with the ordered lamellar nanostructure should be slightly smaller for a linear A−B gradient copolymer than for an A−B diblock copolymer of similar degree of polymerization and overall composition.[39] Further study is needed to determine if the apparent difference between our result and theory in this case is caused by the experiment involving a diblock copolymer consisting of a homopolymer block and a random copolymer block while the theory is for a diblock copolymer consisting of two distinct homopolymer blocks or whether it has a different origin.
(79) Kahle, S.; Korus, J.; Hempel, E.; Unger, R.; Höring, S.; Schröter, K.; Donth, E. *Macromolecules* **1997**, *30*, 7214–7223.
(80) Penzel, E.; Riger, J.; Schneider, H. A. *Polymer* **1997**, *38*, 325–337.
(81) Lipson, J. E.; Milner, S. T. *J. Polym. Sci., Part B: Polym. Phys.* **2006**, *43*, 276–279.
(82) Sun, X. Y.; Luo, Y. W.; Wang, R.; Li, B. G.; Liu, B.; Zhu, S. P. *Macromolecules* **2007**, *40*, 849–859.
(83) Zheng, W.; Simon, S. L. *J. Polym. Sci., Part B: Polym. Phys.* **2008**, *46*, 418–430.
(84) Ellison, C. J.; Torkelson, J. M. *Nat. Mater.* **2003**, *2*, 695–700.
(85) Weidisch, R.; Ensslen, M.; Michler, G. H.; Fischer, H. *Macromolecules* **1999**, *32*, 5375–5382.

(86) Fava, D.; Fan, Y. S.; Kumacheva, E.; Winnik, M. A.; Shinozaki, D. M. *Macromolecules* **2006**, *39*, 1665–1669.
(87) Fay, J. J.; Murphy, C. J.; Thomas, D. A.; Sperling, L. H. *Polym. Eng. Sci.* **1991**, *31*, 1731–1741.
(88) The dispersities or PDIs of our gradient, blocky gradient and blocky random copolymer materials range from 1.2 to 1.5 (with only the S*grad*TBA67 case falling above 1.5); these are in line with expectations for polymers and copolymers prepared using these initiators.[6,18−20,58] The block copolymer material PDIs range from 1.30 for S*block*AS67 to 1.81 for S*block*TBA54. While some block copolymer PDIs are higher than expected for these syntheses, the variation in PDI values is not expected to have an experimentally significant influence on block copolymer T_g breadths or values. The random copolymer PDIs are as expected for materials synthesized using conventional radical polymerization. See Supporting Information for the full list of PDIs.